In Vivo Imaging of Virological Synapses

Xaver Sewald[1], David G. Gonzalez[2], Ann M. Haberman[2], and Walther Mothes[1]*

[1]Department of Microbial Pathogenesis, Yale University School of Medicine, New Haven, CT 06510

[2]Department of Laboratory Medicine, Yale University School of Medicine, New Haven, CT 06510

*Correspondence to: walther.mothes@yale.edu

Walther Mothes

Email: walther.mothes@yale.edu

Phone: 203 737-2203 Fax: 203 737-2630

Department of Microbial Pathogenesis

Yale University School of Medicine

295 Congress Ave, BCMM 335

New Haven, CT 06536, USA

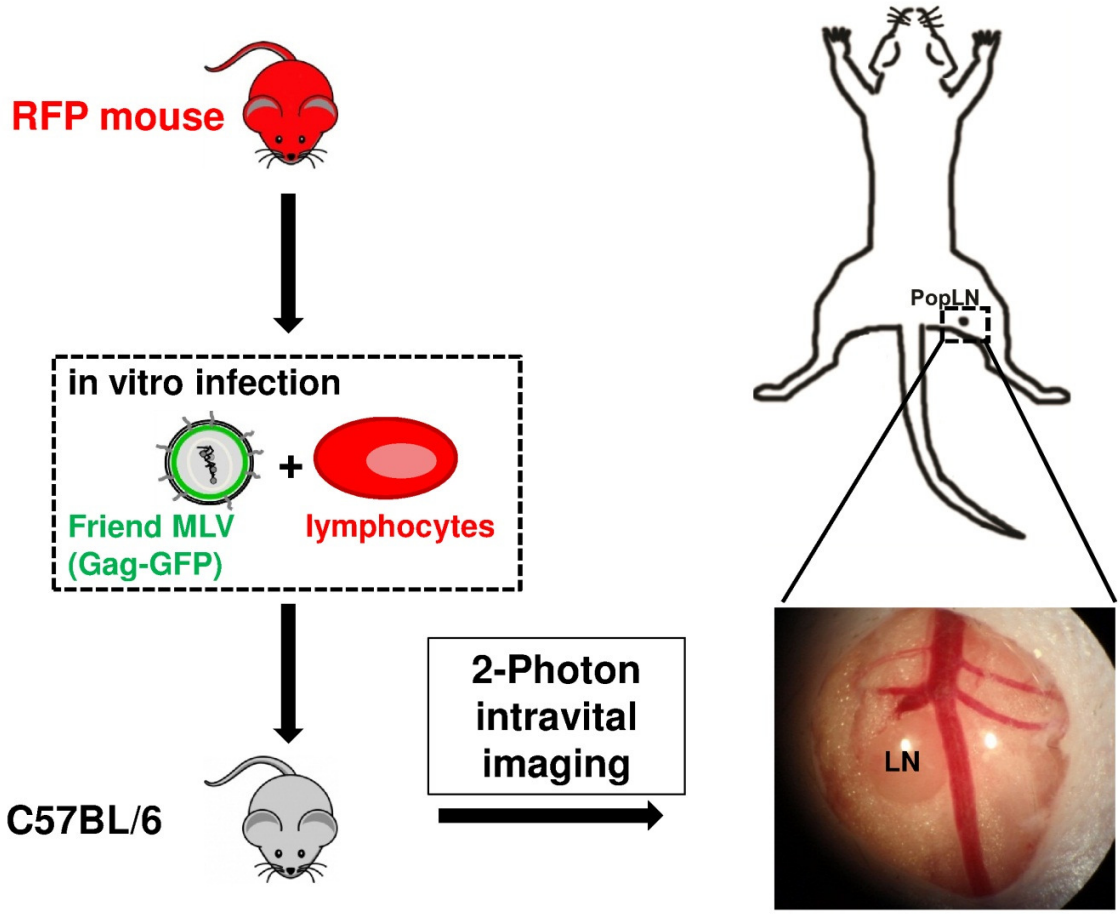

Supplementary Figure S1: Intravital microscopy of F-MuLV-infected lymphocytes. Lymphocytes prepared from strains of mice expressing cytoplasmic RFP (Tg(CAG-DsRed*MST)1Nagy/J) (red) were infected *ex vivo* with F-MuLV Gag-GFP (green). Infected cells generating Gag-GFP labeled virions were reintroduced into 8-12 week old C57BL/6 mice and cells monitored 16-24 h after transfer by intravital microscopy within the popliteal lymph node of the right limb.

a

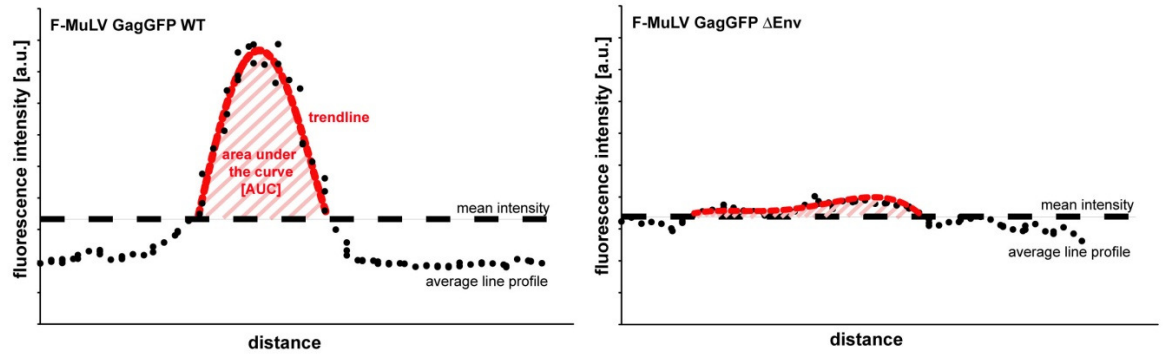

b

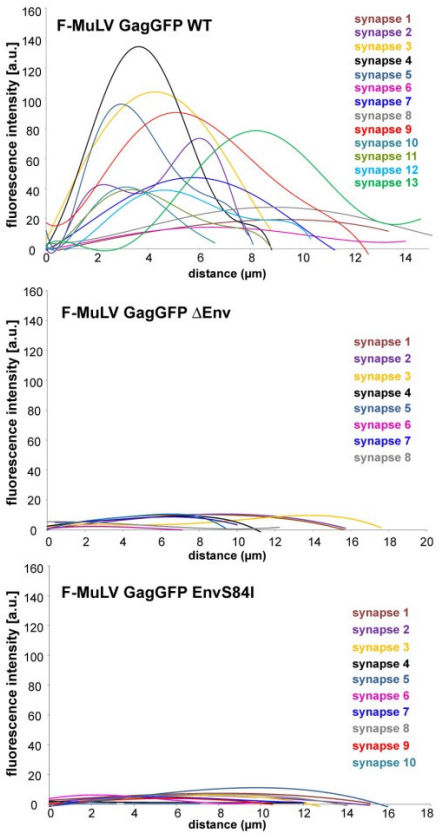

c

curve equation		area under the curve (AUC)
F-MuLV GagGFP WT		
synapse 1:	$y = -0{,}0008x^4 + 0{,}0097x^3 - 0{,}2185x^2 + 4{,}2563x - 2{,}9481$	177
synapse 2:	$y = 0{,}0664x^6 - 1{,}5977x^5 + 14{,}132x^4 - 55{,}876x^3 + 92{,}78x^2 - 30{,}779x - 0{,}0416$	361
synapse 3:	$y = 0{,}076x^4 - 1{,}2085x^3 + 0{,}7459x^2 + 36{,}002x + 5{,}6686$	604
synapse 4:	$y = -0{,}0177x^6 + 0{,}3816x^5 - 2{,}4568x^4 + 2{,}5764x^3 + 10{,}648x^2 + 26{,}495x + 1{,}1295$	583
synapse 5:	$y = 0{,}025x^5 - 0{,}8084x^5 + 9{,}7644x^4 - 53{,}965x^3 + 127{,}24x^2 - 72{,}348x + 12{,}199$	408
synapse 6:	$y = 0{,}0043x^4 - 0{,}1031x^3 + 0{,}4395x^2 + 2{,}6023x - 0{,}563$	122
synapse 7:	$y = 0{,}0202x^4 - 0{,}4722x^3 + 1{,}98x^2 + 8{,}7502x - 0{,}8696$	321
synapse 8:	$y = 0{,}0039x^4 - 0{,}1403x^3 + 1{,}2632x^2 - 0{,}1611x + 3{,}3754$	289
synapse 9:	$y = -0{,}0113x^5 + 0{,}3898x^4 - 4{,}6837x^3 + 20{,}535x^2 - 12{,}638x + 17{,}334$	633
synapse 10:	$y = 0{,}393x^4 - 5{,}1541x^3 + 17{,}559x^2 - 3{,}8181x + 1{,}3273$	148
synapse 11:	$y = -0{,}0386x^5 + 0{,}8728x^4 - 6{,}7089x^3 + 17{,}855x^2 - 0{,}8261x + 0{,}2363$	194
synapse 12:	$y = -0{,}0018x^6 + 0{,}0374x^5 - 0{,}1207x^4 - 1{,}8098x^3 + 12{,}054x^2 - 10{,}139x + 0{,}8983$	250
synapse 13:	$y = -0{,}001x^6 + 0{,}0484x^5 - 0{,}8402x^4 + 6{,}1392x^3 - 16{,}424x^2 + 12{,}651x + 2{,}2345$	724
F-MuLV GagGFP ΔEnv		
synapse 1:	$y = -0{,}0009x^4 + 0{,}0267x^3 - 0{,}4072x^2 + 3{,}193x + 0{,}8334$	114
synapse 2:	$y = -0{,}0071x^3 + 0{,}0182x^2 + 1{,}5015x + 0{,}8176$	114
synapse 3:	$y = -0{,}0018x^4 + 0{,}051x^3 - 0{,}4042x^2 + 1{,}1843x + 2{,}3145$	105
synapse 4:	$y = -0{,}0047x^4 + 0{,}0723x^3 - 0{,}435x^2 + 2{,}0716x + 2{,}4933$	73
synapse 5:	$y = -0{,}014x^4 + 0{,}2183x^3 - 1{,}3055x^2 + 4{,}7186x + 0{,}2198$	70
synapse 6:	$y = 0{,}0166x^3 - 0{,}3076x^2 + 1{,}2193x + 0{,}9595$	11
synapse 7:	$y = -0{,}0347x^3 + 0{,}3671x^2 - 0{,}372x + 5{,}1899$	69
synapse 8:	$y = 0{,}0119x^3 - 0{,}1858x^2 + 0{,}1905x + 5{,}4834$	35
F-MuLV GagGFP EnvS84I		
synapse 1:	$y = -0{,}0042x^3 - 0{,}0041x^2 + 0{,}8937x + 2{,}6504$	83
synapse 2:	$y = 0{,}0022x^3 - 0{,}1471x^2 + 1{,}6159x + 1{,}0851$	60
synapse 3:	$y = -0{,}0156x^3 + 0{,}1475x^2 + 0{,}5046x + 0{,}4818$	46
synapse 4:	$y = 0{,}0071x^2 - 0{,}1571x + 1{,}8411$	15
synapse 5:	$y = -0{,}0014x^2 + 0{,}0453x + 0{,}3473$	3
synapse 6:	$y = 0{,}0435x^3 - 0{,}7041x^2 + 2{,}4638x + 3{,}7375$	35
synapse 7:	$y = 0{,}0158x^3 - 0{,}417x^2 + 2{,}9537x - 1{,}446$	37
synapse 8:	$y = -0{,}0056x^3 - 0{,}0269x^2 + 1{,}426x + 0{,}1136$	63
synapse 9:	$y = -0{,}0037x^3 - 0{,}0829x^2 + 1{,}2885x - 0{,}0783$	27
synapse 10:	$y = -0{,}0128x^3 + 0{,}1204x^2 + 1{,}3072x - 1{,}2281$	102

Supplementary Figure S2: Defining a Gag polarization coefficient. a) To define a parameter that describes the extent of Gag polarization with respect to its intensity, width and duration, the space under the polygonal best fit trendline (area under the curve, AUC) of each average polarization line profile represented in Fig. 2d was determined by integration. The AUC as a measurement for the polarization coefficient is presented in Fig. 2e. Best fit trendlines for all quantified cells infected with F-MuLV Gag-GFP WT, F-MuLV ΔEnv and F-MuLV Gag-GFP EnvS84I are shown in b) and integrated curves with values for AUC are listed in c).

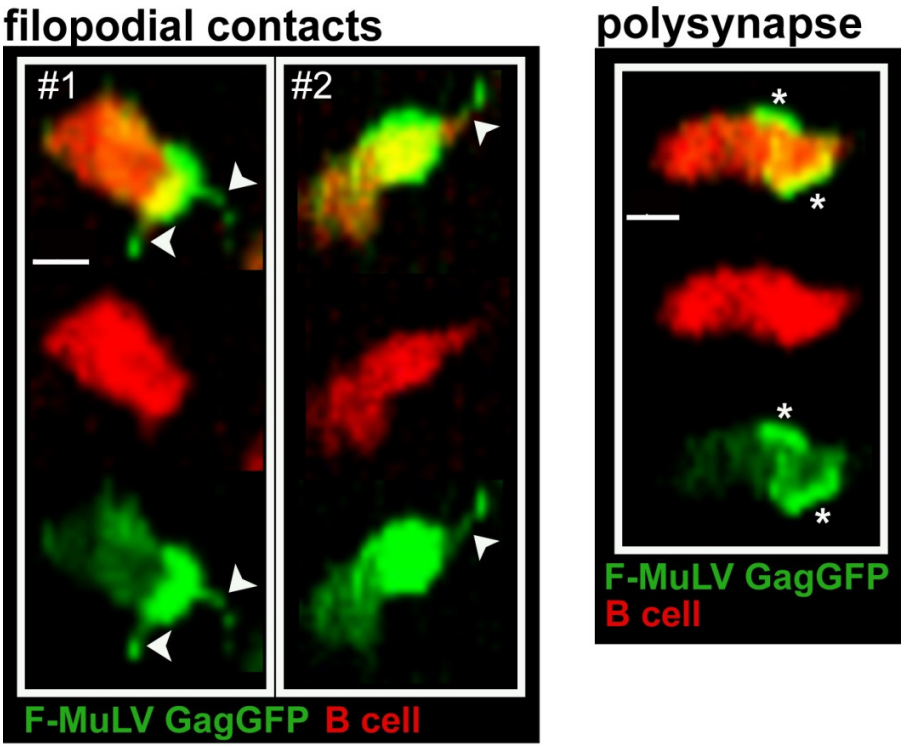

Supplementary Figure S3: *In vivo* detection of filopodial bridges and polysynapses. Individual images from movie sequences as shown for Supplementary Movie 3 with filopodial contacts and polysynapses of B cells carrying Gag-GFP-labeled material. The arrowheads depict filopodial contacts and the stars depict virological synapses. Scale bars represent 5µm.

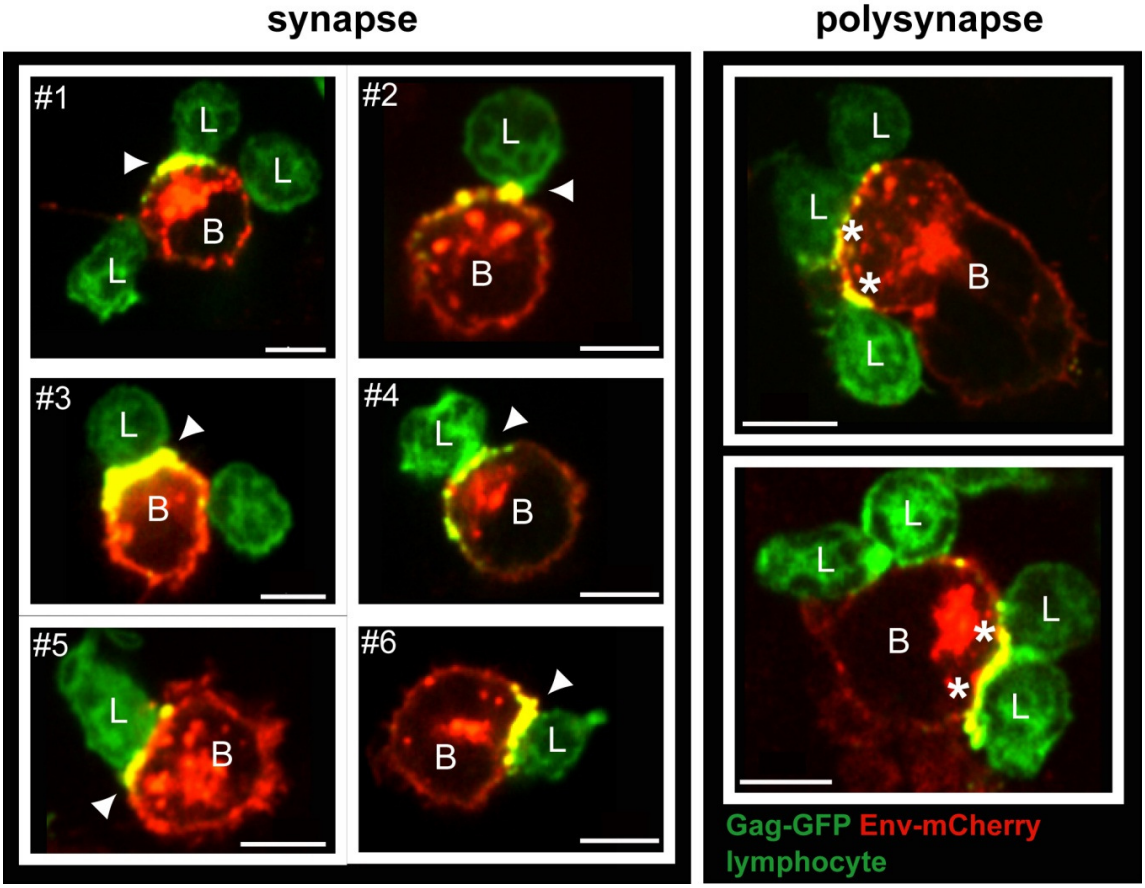

Supplementary Figure S4: F-MuLV-infected B cells form virological synapses *in vitro*. F-MuLV (green, Gag-GFP; red, Env-mCherry) infected B cells (B) were co-cultured for 12 h with total leukocytes isolated from popliteal and inguinal lymph nodes (L, green). Co-cultures were fixed and imaged using spinning disc confocal microscopy. Arrowheads and stars indicate virological synapses and polysynapses. Scale bars represent 5µm.

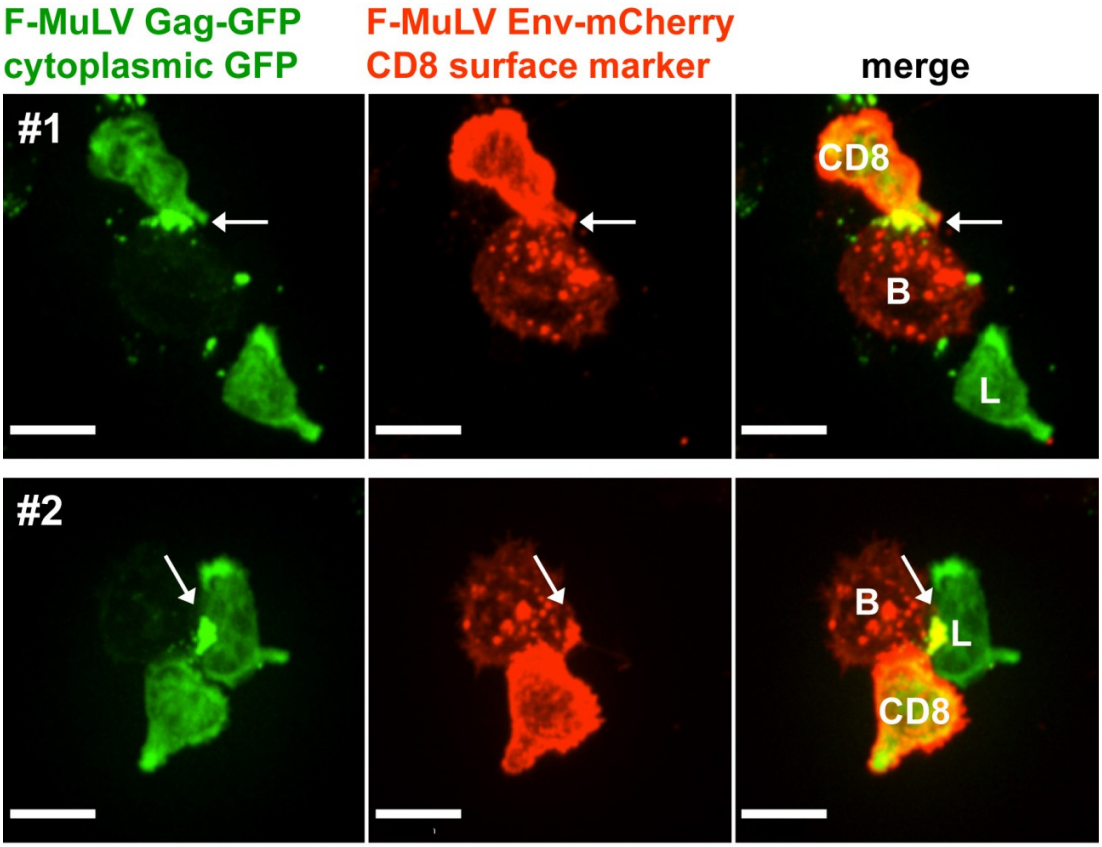

Supplementary Figure S5: Identification of target cells for F-MuLV-infected B cells by surface marker staining. F-MuLV (green, Gag-GFP; red, Env-mCherry) infected B cells (B) were co-cultured for 12 h with total leukocytes (L) expressing cytoplasmic GFP isolated from popliteal and inguinal lymph nodes (green). Co-cultures were fixed and stained with antibodies against different surface markers (red). Two examples for surface staining against CD8 are shown. Arrows indicate virological synapses. Scale bars represent 7µm.

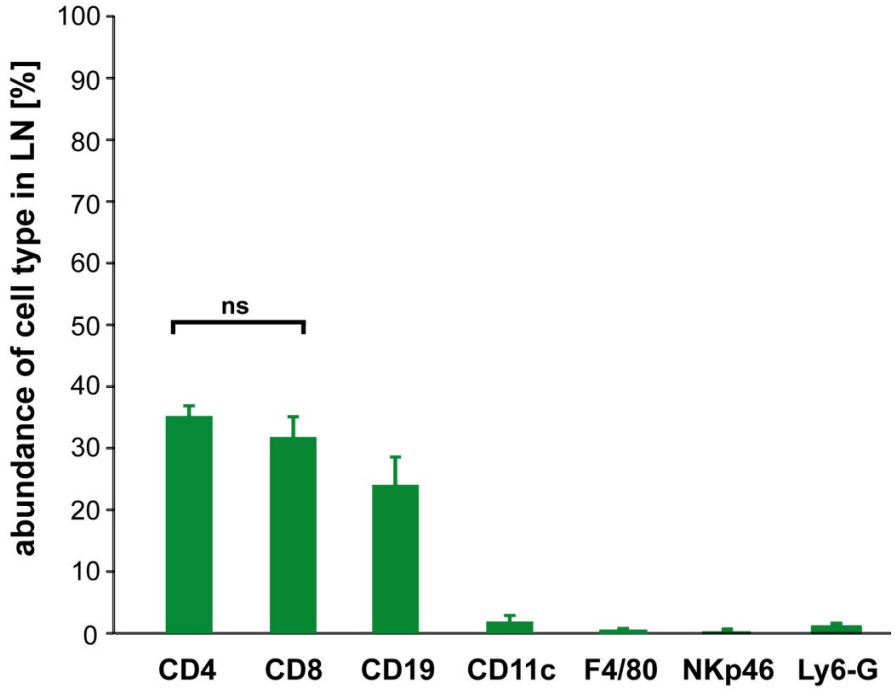

Supplementary Figure S6: Abundance of cell types in lymph nodes. Leukocytes from pooled inguinal and popliteal lymph nodes of cytoplasmic GFP-expressing Tg(UBC-GFP)30Scha/J mice were stained with antibodies for surface markers and analyzed by flow cytometry. Data are the mean±s.d. of three independent experiments. CD4 compared to CD8: $^{\text{ns (non-significant)}}$P=0.185 (unpaired t-test).

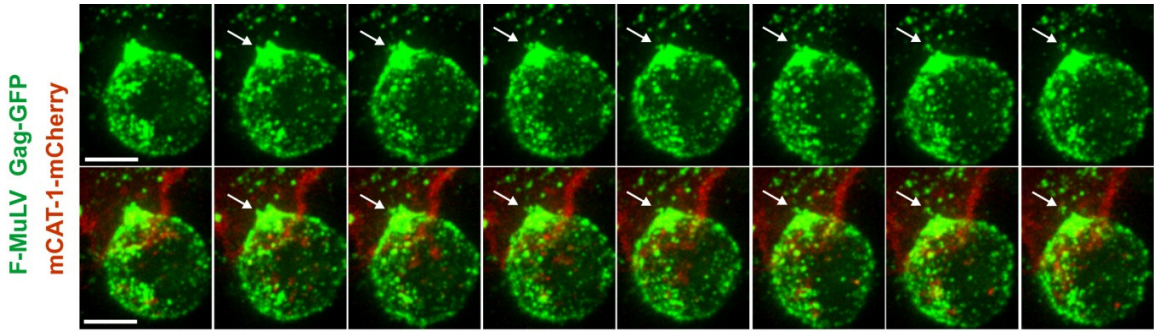

Supplementary Figure S7: Transfer of F-MuLV from infected primary B cells to receptor-expressing XC target cell. B cells from C57BL/6 mice were infected with F-MuLV Gag-GFP and co-cultured with adherent XC cells expressing mCAT-1-mCherry. Viral particles are transferred over cell-cell contacts characterized by the accumulation of Gag-GFP and mCAT-1-mCherry. Images represent extended focus projections (z-spacing of 0.5 µm) and are acquired every 59 seconds. Whole transfer is shown in Supplementary Movie 7. Arrows depict transfer of viral particles. Scale bars represent 3µm.

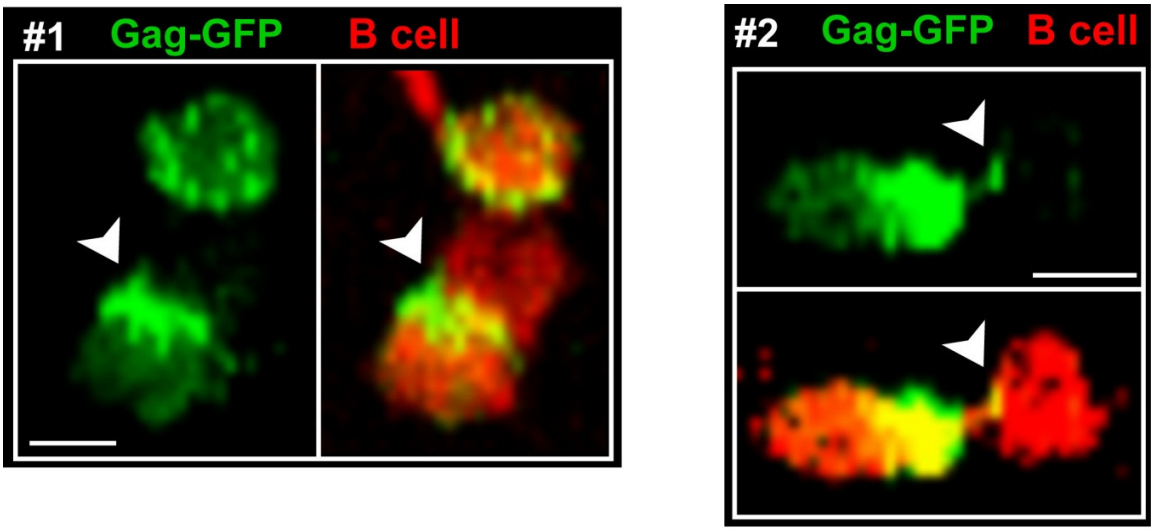

Supplementary Figure S8: *In vivo* detection of virological synapses between B lymphocytes. Individual images from intravital microscopy experiments of F-MuLV Gag-GFP-infected B cells in the popliteal lymph node of C57BL/6 mice. Arrowheads depict Gag-GFP polarization of virological synapses (#1) or filopodial contacts (#2) observed between F-MuLV-infected (red/green) and uninfected B cells (red). Image sequence of synapse #1 is shown as Supplementary Movie 8. Scale bars represent 5µm.

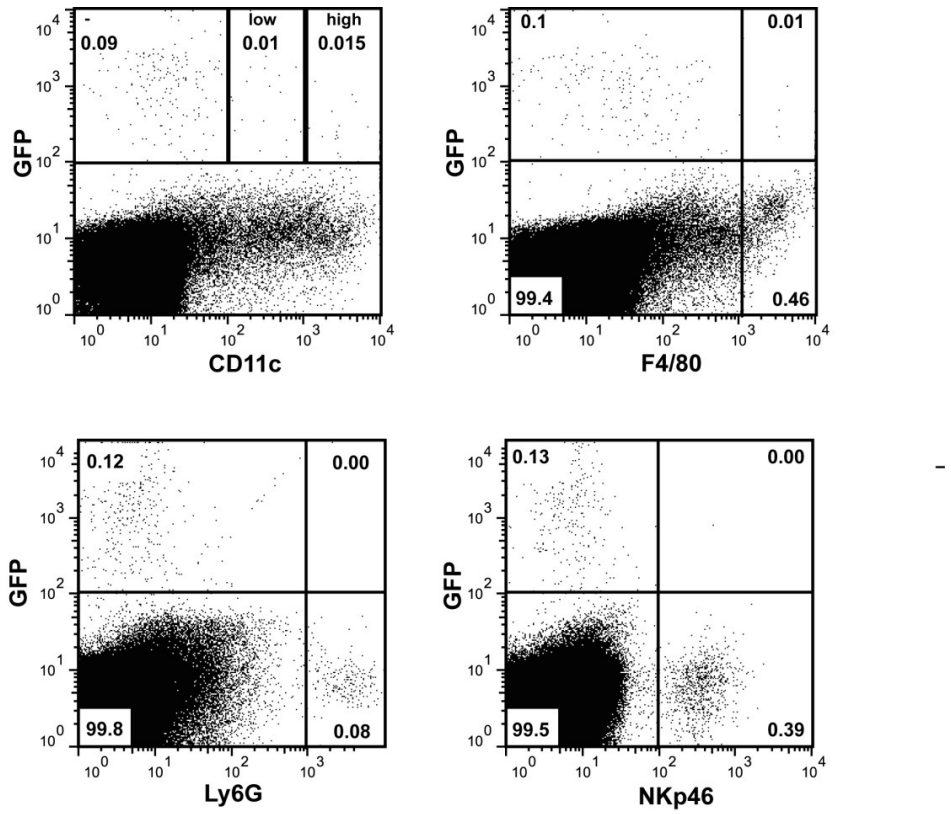

Supplementary Figure S9: Flow cytometry analysis of draining popliteal lymph nodes of F-MuLV-infected mice. C57BL/6 mice were infected with F-MuLV-LTR-GFP ΔEnv by footpad injection and the draining popliteal lymph node was analyzed 2.5 d later by flow cytometry. Fixed leukocytes were stained with antibodies against CD11c, F4/80, Ly6G and NKp46. The parallel corresponding results for antibodies against CD4, CD8 and CD19 are presented in Fig. 4c. Numbers in each square represent percentage to total cells counted.